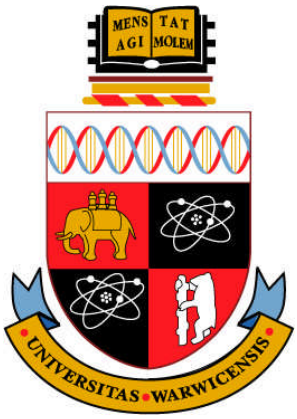

Solid-State NMR Studies Of The M2 *Influenza A* Transmembrane Protein

Adair Richards*

**Molecular Organisation and Assembly in Cells Doctoral Training Centre, University of Warwick, Coventry CV4 7AL, UK*

Supervisor: Dr Steven Brown[†]

Co-Supervisor: Dr Andreas Kukol[‡]

[†] *Department of Physics, University of Warwick, Coventry CV4 7AL, UK*

[‡]*Department of Biological Sciences, University of Warwick, Coventry CV4 7AL, UK*

Table of Contents

List of Figures

Summary

The M2 transmembrane protein tetramerises to form a proton channel on the *Influenza A* virus which is a potential drug target. Here a novel technique, namely solid-state NMR, is used alongside infrared spectroscopy to undertake structural investigations of the transmembrane domain. A synthetic peptide representing this domain was purified and analysed first in isolation and also when reconstituted in a lipid bilayer. An effective methodology for performing solid-state NMR on biological samples was developed using a cross-polarisation magic angle spinning (MAS) technique on isotopically labelled ^{13}C carbonyl groups. Results showed a change in the chemical shift and asymmetry co-efficient in the NMR spectra of the labelled carbonyl groups when in the residue isolated from other types of molecule compared to when it is embedded in a lipid bilayer.

Acknowledgements and Declaration

I would like to thank Steven Brown and Andreas Kukol for their help and guidance during the lifespan of this project and for their constructive feedback on the draft version. I would also like to thank Andrew Beevers and Tran Pham for their assistance during the experimental stages of the project. This work has been funded by the Engineering and Physical Sciences Research Council Life Sciences Initiative.

This thesis has been presented in accordance with the rules and regulations set forth by the University of Warwick Graduate School. It has been composed by myself and not submitted in any previous application for any degree. The work in this thesis has been undertaken by myself except where otherwise stated.

1 Introduction

1.1 M2 and the *Influenza A* Virus

The *Influenza* virus has been the cause of the most deadly disease outbreaks on a global scale in the last 200 years. It is estimated that 5-15% of the world population contract *Influenza* annually with an average death toll of between 250 000 and 500 000. Major pandemics have been known to kill as many as 40 million in a single winter (World Health Organisation, 2003). The most commonly used and most effective antiviral agents currently available that act against *Influenza A* are amantadine (Hay *et al.*, 1985) and rimantadine (Nidus, 2001) which target the M2 proton pathway (see Figure 1) and therefore any progress in high-resolution structural determination of this membrane protein is of significant biomedical importance.

M2 is a tetrameric transmembrane protein consisting of four monomers containing 97 residues (sequence in appendix) with one 19-residue transmembrane helix, a 24-residue extraviral chain and a 54-residue intraviral segment (Holsinger & Lamb, 1991). These four monomers form a tetramer and the resulting complex establishes a H^+ channel involved in endocytosis and exocytosis and hence provides a unique opportunity as a potential drug target. It is thought that M2 is involved in the virus uncoating process which follow viral uptake by endocytosis. H^+ ions travel from a relatively high level of concentration in the endosomal lumen into the virion which weakens the interactions between the ribonucleoprotein (RNP) core and the matrix protein (M1). Amantadine is a blocker of the M2 pathway and, when present, it prevents the completion of the virus uncoating and consequently RNPs are unable to promote infection.

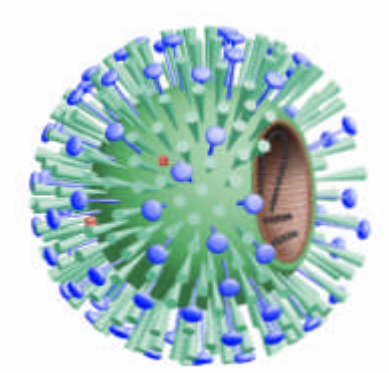

Figure 1: *Influenza A*, M2 pathway in red (Roche, 2004)

In common with other enveloped viruses, *Influenza A* enters a host organism via the endocytotic pathway by attaching itself to the host cell's membrane. Consequently, the host cell incorporates the virus into the membrane and eventually it is tied off to form an intracellular virion. Once in an endosome, the host cell begins to acidify this compartment with ATPases. The virus escapes this

compartment by fusing with the membrane when the membrane protein hemagglutinin undergoes conformational change as a response to the pH being lowered to between 5.0 and 5.5 (reviewed in Fischer *et al.*, 2002). This change in intraviral pH also induces the release of the viral RNA into the host cell and consequently the spread of the virus. It is known that M2 is effectively the only channel which regulates pH within the virus thus making it an obvious drug target.

The aim of this work is to use a novel technique, namely solid-state nuclear magnetic resonance (NMR), as well as infra-red spectroscopy (IR), to investigate the structural characteristics of the M2 transmembrane domain and to develop the methodology for performing solid-state NMR on biological samples. To achieve this, a synthetic 25 residue ^{13}C-labelled peptide representing the transmembrane helix of M2 was analysed using a magic angle spinning (MAS) solid-state NMR technique. More specifically, the labelled peptide was analysed in its raw powdered state and in combination with lipid vesicles in dry and gel-like forms.

1.2 Biological Techniques and Background

Membrane proteins constitute about 30% of all proteins found in cells and 70% of all pharmaceutically relevant proteins but they are among the least well characterised (Otzen, 2004). This is because they are generally expressed in very low levels, they aggregate easily and their hydrophobicity requires an amphiphilic environment to remain soluble. So far only a small number of membrane protein structures have been solved, using X-ray crystallography, NMR and infra-red spectroscopy.

M2 has not been crystallised to date and the most successful structural studies have used solid-state NMR and Fourier transform infra-red (FTIR) spectroscopy. Initial circular dichroism (CD) experiments (Duff *et al.*, 1992) on synthetically generated transmembrane 25-residue peptide indicated a stable α-helical structure when reconstituted into 1,2-dioleoyl-sn-glycero-3-phosphocholine liposomes although similar experiments using 1,2-dioleoly-sn-glycero-3-phosphoglycerol liposomes resulted in a less clear structure. A later study (Kochendoerfer *et al.*, 1999) showed that approximately 40 residues encompassing the transmembrane domain form an

α-helix when reconstituted in dodecylphosphocholine micelles which remain when the protein tetramerises.

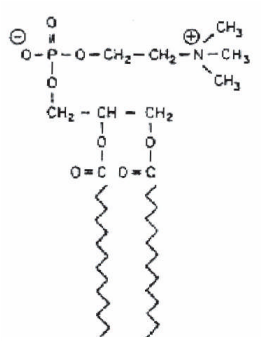

Figure 2: DPPC

The peptides are reconstituted in lipids (see Figure 2) to mimic *in vivo* conditions where the hydrophobic transmembrane domain is embedded among the tails of the hydrophobic lipids which naturally form a bilayer in the presence of water. The hydrophilic tails either side of the transmembrane will naturally exist outside of the lipid bilayer.

A valuable technique in this area that has arisen recently is the use of site-specific infra-red dichroism (SSID) (Arkin *et al.*, 1997) as a basis for restraints on molecular dynamics protocols. Infrared spectroscopy dichroism measurements of single amide I vibrational modes which correspond to ^{13}C-labelled sites within a peptide contain information about the helix tilt and rotation angles which may be extracted by analysing the dichroism of a set of labelled sites (2 are sufficient) along the peptide sequence. This uses the ability to measure selectively the infrared absorption of a particular mode in the peptide where the ratio of the dichroism gathered from using polarised light can be directly related (Torres *et al.*, 2001) to the orientation of the transition dipole moment and hence to the bond orientation of the particular chromophore.

1.3 The NMR Phenomenon

NMR is a powerful technique which can reveal sub-molecular information based on a property of nuclei known as spin. The spin of a nucleus refers to an intrinsic quantum physical property of a nucleus which has no direct comparison in the macroscopic world and behaves like an angular momentum. Scientists were forced to postulate its existence and the NMR phenomenon is one of the clearest demonstrations for the validity of spin. Nuclear spin has only a negligible effect on the chemical and physical properties of atoms but fluctuations in spin orientation can be recorded by sensitive spectrometer apparatus. Spin results in giving angular momentum to a particle which

can be quantized and is equal to $\hbar\sqrt{I(I+1)}$ where I is the spin quantum number which can be a non-negative integer for particles called bosons or a positive half-integer in the case of fermions.

The spin of an atom is the sum of the spin of its neutrons, protons and electrons, which in turn is equal to the sum of the spins of the quarks and leptons. Within a nucleon, the spins of two quarks are antiparallel with the third quark having a spin parallel to one of the other quarks giving a net spin of ½. The electron being a single fundamental particle also has a spin of ½. The isotope utilised in this work is ^{13}C which has a net spin of ½ (the natural isotope ^{12}C with one less neutron has spin 0), this is because the spins of the nucleons naturally align themselves in antiparallel positions in the ground state.

One of the problems with studying ^{13}C in samples is the relatively low (1.1%) natural abundance of ^{13}C which results in a difficulty in getting enough NMR signal and so isotopically labelled ^{13}C samples are used. (This is in contrast to IR where only a very small amount of sample is required to produce a signal.) However, the natural abundance ^{13}C from other carbon groups in the sample can complicate the analysis of results if there are a significant number of carbon atoms in the sample. Although isotopomers can produce vastly different NMR signals, they show very little variation in their chemical and physical properties and so in most cases an isotopically labelled biological sample can be considered identical to the wild type sample.

Nuclear spin results in an intrinsic magnetic moment of nuclei. This magnetic moment is proportional to spin angular momentum and the constant of proportionality is termed the magnetogyric ratio. This ratio may be positive which results in the magnetic moment being parallel to the angular momentum or it may be negative in which case the magnetic moment is antiparallel to the direction of angular momentum. This has a bearing on the spin polarisation axis which is the direction of the spin angular momentum. When a nucleus is placed in an external magnetic field, its magnetic moment will align parallel to the direction of the external magnetic field in order to minimise the magnetic energy and the polarisation axis precesses around the direction of the field. The angle of precession depends solely on the initial spin polarisation. The frequency which the spin precesses is called the Larmor frequency and is directly proportional to the strength of the magnetic field experienced by the particle with the

constant of proportionality being the magnetogyric ratio. A positive ratio results in a clockwise precession when viewed against the direction of the field and similarly a negative magnetogyric ration results in an anticlockwise precession.

As well as the external magnetic field, every particle experiences a constantly fluctuating microscopic magnetic field as a result of the electrons and nuclei surrounding it. This microscopic field fluctuates rapidly because of the thermal motion of the environment and may be in any direction. Thus the resulting total magnetic field a particle experiences has a slightly fluctuating magnitude, direction and Larmor frequency. The fluctuating fields cause a gradual cessation of the constant-angle precession of the nuclear spins. For each particle, the angle between the spin magnetic moment and the external magnetic field varies slightly which results in the direction of the magnetic moment of each nuclear spin changing and eventually sampling the entire range of possible orientations (see Figure 3). This wandering motion is anisotropic as, for a finite temperature, it is slightly more probable (10 001 spins parallel to the field for every 10 000 spins in each other direction), that the nuclear spin is in the direction of lowest magnetic energy i.e. parallel to the external magnetic field than any other direction and this provides the basis for gathering information by spectrometers (Levitt, 2000).

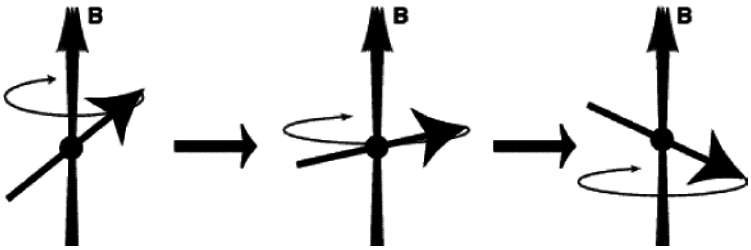

Figure 3: Precession in a fluctuating field (Levitt, 2000)

The anisotropy of the magnetisation distribution in thermal equilibrium that results in the entire sample acquiring a small net longitudinal magnetic moment is called the microscopic mechanism of nuclear paramagnetism. This is about four degrees of magnitude smaller than the dimagnetism due to the electrons present. It is very difficult to measure the magnetic field strength in the direction of the external field and elicit information about the nuclear paramagnetism. Instead, a more indirect approach has been developed.

A radiofrequency pulse which is an oscillating magnetic field is applied for the appropriate duration at the appropriate frequency which causes all the spin polarisations to rotate by 90˚.

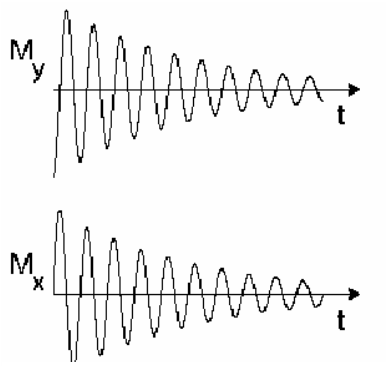

Figure 4: Decay and oscillation of transverse magnetism (Levitt, 2000)

When the pulse is switched off, a net spin polarisation exists perpendicular to the external field and since each individual spin precesses, the bulk magnetic moment does as well. The precession frequency of this bulk moment is the same as the Larmor frequency. (Note that quantum mechanically we are only able to specify the magnitude and direction in one dimension of the spin polarisation.) When the pulse is switched off, there is a net poarisation perpendicular to the external field and since each spin precesses, the bulk magnetic moment precesses as well, also in the plane normal to the external field axis. This transverse magnetic moment decays or 'relaxes' over time approximately exponentially and in an oscillating manner (see Figure 4).

The transverse bulk magnetic moment is very weak but it oscillates at a well-defined frequency and can be reliably detected. This is achieved by placing a wire coil in close proximity to the sample and an oscillating electric current is induced in the wire from the changing magnetic field it experiences (see Figure 5). This current can then be detected with a sensitive radiofrequency detector and is referred to as the NMR signal or free-induction decay.

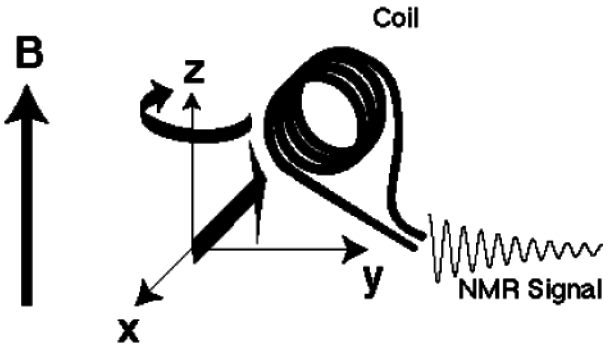

Figure 5: Induction of an NMR signal (Levitt, 2000)

This technique delivers information on a submolecular scale to a high resolution because of the inhomogeneous distribution of electrons in molecules. Most of the electrons are situated in chemical bonds between nuclei or very close to the nuclei and therefore the spins at different points within the molecule are subject to slightly different magnetic fields. This effect of a change in the resonance frequency due to its local chemical environment is termed the chemical shift. This is displayed as a resonance peak at a particular parts per million (ppm) value on an (already Fourier-transformed) NMR spectrum.

So, in summary an NMR spectrometer operates by applying a large magnetic field to a sample which magnetises the spins, applying a radiofrequency pulse at the Larmor frequency to rotate the spin polarisations and produce a transverse bulk magnetic moment, and then detecting the small electric currents induced by this moment.

1.4 CP MAS Solid-State NMR

Solid-state NMR is different to solution-state NMR because the nuclei are not tumbling around one another. In solution-state NMR, the effect of the tumbling nuclei is an averaging of chemical shift anisotropy and dipole-dipole couplings and the overall isotropy results in narrower band-widths and larger signal amplitudes. This is because the orientation of the nuclei with respect to the external field changes on a timescale that is faster than the inverse anisotropy of the interactions.

The lower resolution and sensitivity of solid-state NMR due to these intrinsic properties were greatly improved by spinning the sample at the magic angle of 57.4° with respect to the external field direction (Lowe, 1959). At this angle $\theta_{MA} = a\cos\sqrt{\frac{1}{2}}$, the second Legendre polynomial, $\frac{1}{2}\left(3\cos^2\theta - 1\right)$, is equal to zero. This results in a strengthening of the FID and a narrowing of the line-widths. The rotation frequencies used are usually slightly smaller than the spectral width of the lines ranging from 2-20KHz for a 4mm rotor. Heteronuclei such as ^{13}C require only a small rotation frequency to narrow the spectral width because most of the broadening is a consequence of dipole-dipole coupling and chemical shift anisotropy. Hence, a further increase in rotation frequency results in a decrease in the number of side bands evident with little further effect on line widths.

One further method of increasing NMR signal is a double resonance technique called cross-polarisation (CP). In this technique, which was applied in this study, a transverse magnetisation is

first induced on the protons and then a further pulse is applied to both the protons and the carbons resulting in a transfer of magnetism to the carbons. The disadvantage of this technique is that the resulting peak heights are no longer quantitative.

This technique is often combined with two particle phase modulation (TPPM) decoupling (Bennett *et al*., 1995) which decouples the protons during FID detection. A diagram illustrating the pulse sequence is given below in Figure 6.

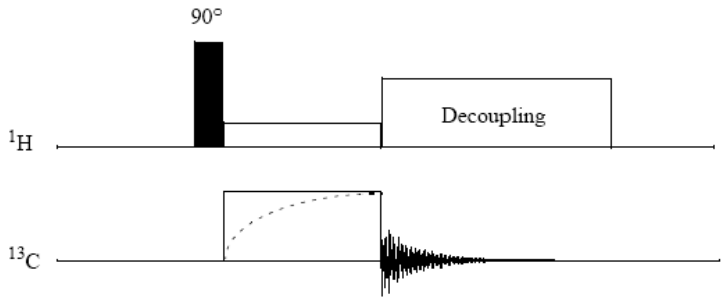

Figure 6: Pulse Sequence for a CP NMR experiment (Jeschke, 2003)

2 Materials and Methods

Four synthetically generated peptides with 25 residues (Influenza strain A/Udorn/307/72 residues Serine22-Leucine46) were made by standard solid-phase F-moc chemistry, cleaved from the resin with hydrofluoric acid and lyophilised (Advanced Biotechnology Centre, Imperial College School of Medicine, London, UK). The sequence can be found in appendix. The peptides had ^{18}O and ^{13}C labels on Isoleucine35, Leucine36, Leucine38 and Isoleucine39 on samples AK01-04 respectively (see Figure 7). The ^{18}O labels have no effect on the resulting NMR spectra and are present only for the benefit of future IR and NMR experiments. Experiments were carried out on all samples but the results given below refer to work with AK02 unless otherwise stated.

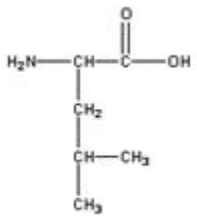

Figure 7: Leucine

2.1 Peptide Purification

The peptide was dissolved in 2ml of trifluoroacetic acid (TFA) and injected immediately onto a high performance liquid chromatography (HPLC) column (Jupiter 5u C4 300R, No. 79744-1, Phenomex, Cheshire, UK) after its equilibration with 90.4% H_2O, 5.7% isopropanol, 3.8% acetonitrile and 0.1% TFA for 10 minutes at 1ml/min. The peptide was eluted using a linear gradient controlled by Biocad software (Biocad Sprint, Perceptive Biosystems, USA). Pooled fractions were frozen in liquid N_2 and subjected to high vacuum (RV3, No. 006840503, BOC Edwards, Crawley, UK) for 24 hours.

2.2 Peptide Reconstitution into Lipid Vesicles

20mg of M2 peptide (M_r=2731) was reconstituted into 134mg of 1,2-dipalmitoly-sn-glycero-3-phosocholine (DPPC) (M_r=734.05) (Lot 160 PC-236, Avanti Polar-Lipids Inc, Alabaster, USA) in a ratio of 1 molecule of M2 peptide to 25 molecules of DPPC. The DPPC was dissolved in 2ml of 1,1,1,3,3,3-hexafluor-2-proponol (Ridel-de Haen, Seelze, Germany) and added to the M2 peptide. The solvent was removed by rotational evaporation (R-3000 Rotavapor, Buchi, Switzerland) and the residue was kept under high vacuum (RV3, No. 006840503, BOC Edwards, Crawley, UK) for 16 hours. 13ml of H_2O was added and the containing flask then sonicated for 2

minutes and then freeze-thawed 3 times using liquid N_2. The solvent was then evaporated off by being frozen in liquid N_2 and placed statically under a high vacuum for a period of 24 hours.

2.3 Hydration of the Peptide/Lipid Mixture

The peptide (AK03) was reconstituted into DPPC as described above. Two samples were prepared by adding 200µl/400µl H_2O to 30mg of peptide. These were then vortexed for 10-15 seconds (Whirlimixer, Fisher Scientific UK Ltd, Loughborough, UK), sonicated for 1 minute, vortexed again for 10-15 seconds and then exposed to a freeze-thaw cycle three times.

2.4 Infrared Spectroscopy

FTIR of the M2 (AK03) in a DPPC bilayer was recorded on a Bruker Vector 22 (Bruker Optik GmbH, Ettlingen, Germany) using the software OPUS (Version 3.1, Bruker Optik GmbH, Ettlingen, Germany) and analysed using GRAMS/AI (Version 7.00, Thermo Galactic, Woburn, USA). 250µl of H_2O was added to 15mg of the AKO2 and DPPC powder produced by the above method. The sample was then vortexed for 30 seconds (Whirlimixer, Fisher Scientific UK Ltd, Loughborough, UK), sonicated for 1 minute and freeze-thawed once. Two drops of the sample were then applied to a CaF_2 disk using a pipette (P100, Gilson Inc., Middleton, USA). Nitrogen was then blown over the surface for 15 minutes and then subjected to vacuum for 10 minutes (RV3, No. 006840503, BOC Edwards, Crawley, UK) and blown with a standard hairdryer for 10 minutes. This was so as to dry the sample sufficiently for FTIR. Background and sample spectra were taken in the usual manner under a high level of N_2 purging. Peak fitting was applied to the spectra using a mixed Gaussian and Lorentzian algorithm (Press *et al.*, 1986) with medium sensitivity and the maximum possible peaks constraint was set to 6.

2.5 Solid-state MAS NMR

Solid-state NMR measurements were performed on a 600MHz spectrometer using a Chemagnetics data acquisition system (CMX Infinity, Chemagnetics, For Collins, USA), a Magnex magnet (600/89, No. 973325,Magnex Scientific Ltd, Yarnton, UK) and using Spinsight software (Version 4.1, Varian Associates Inc, Palo Alto, USA). All the samples were loaded into a 4mm Zaconian rotor with standard packing tools and placed inside a 4mm probe (T3 4mm, No. 700.3, Varian Associates Inc, Palo Alto, USA) except the L-Leucine sample (Lancaster Synthesis

Ltd, Morecambe, UK) which was placed inside a 3.2mm rotor and probe (T3 3.2mm, No. 701.1, Varian Associates Inc, Palo Alto, USA) and the gel-like samples which were loaded into specially adapted rotors which an extra insert to prevent the cap dislodging during rotation (NMR Spectroscopy Facility, Oxford University, UK). A fresh mark with a black marker pen was placed on one side of the top of each rotor to increase the accuracy of the tachometer. The probe was double-tuned to the resonant frequencies of ^{1}H at 600.1MHz and ^{13}C at 150.9MHz initially using a network analyser (RF Network Analyser, No. 8712ET, Agilent Technologies Inc, Palo Alto, USA) and then by oscilloscope (Infinium Oscilloscope, Ref. US3813921, Hewlett-Packard, Palo Alto, USA). The forward to backward power ratios for both ^{1}H and ^{13}C were at least 10 in every reading. The shim magnets were set using a standard program (MAS4N_0104, Brown, University of Warwick, UK). The chemical shifts were calibrated using a standard sample of L-Alanine. Results were obtained using a ramped cross-polarisation method with TPPM decoupling.

3 Results

3.1 NMR Spectra

Figures 8 and 9 show the spectra of the M2 peptide in an unpurified powder form with a strong carbonyl signal at 176.6ppm.

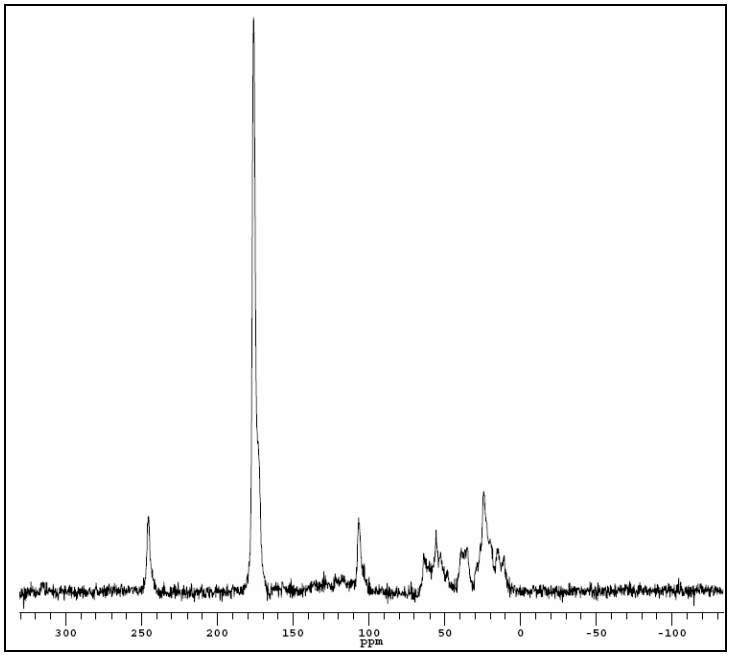

Sample Name	M2 peptide (AK02)
MAS Frequency	10.4KHz
No. of Acquisitions	320
Pulse Delay	1.5s
Acquisition Time	14.29ms
90° ^{1}H Pulse Length	2.5µs
Contact Time	2.5ms

Figure 8: M2 Peptide

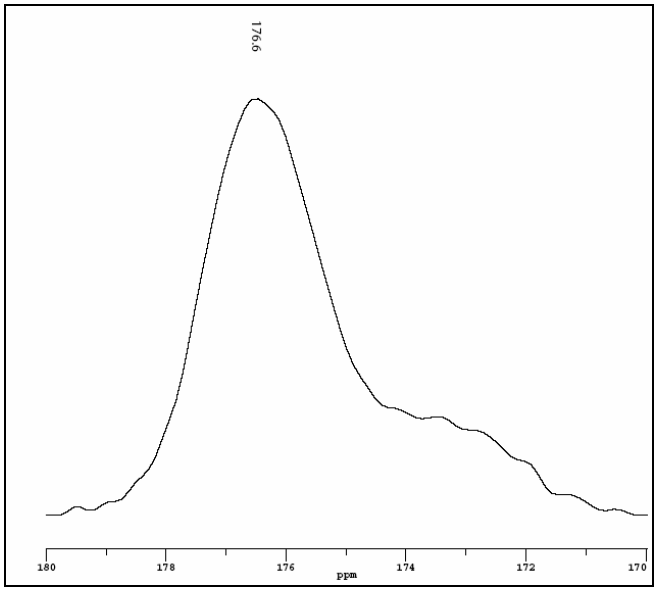

Sample Name	M2 peptide (AK02)
MAS Frequency	10.4KHz
No. of Acquisitions	320
Pulse Delay	1.5s
Acquisition Time	14.29ms
90° ^{1}H Pulse Length	2.5µs
Contact Time	2.5ms

Figure 9: M2 Peptide, expanded carbonyl region

Figure 10 shows the spectra from unlabelled L-Leucine with a carbonyl doublet at 176.3 and 177.2ppm. Figure 11 shows the carbonyl region of L-Leucine spinning at 3.1KHz.

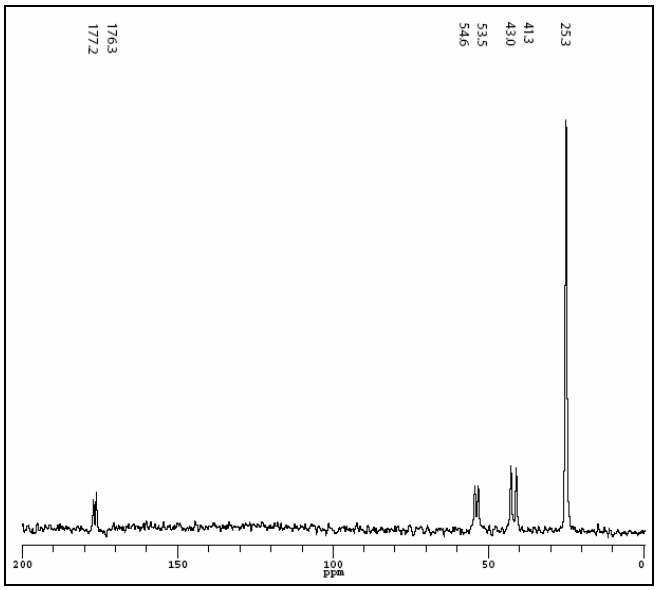

Sample Name	L-Leucine
MAS Frequency	10.1KHz
No. of Acquisitions	128
Pulse Delay	3s
Acquisition Time	20ms
90° ^{1}H Pulse Length	2.5µs
Contact Time	1ms

Figure 10: L-Leucine

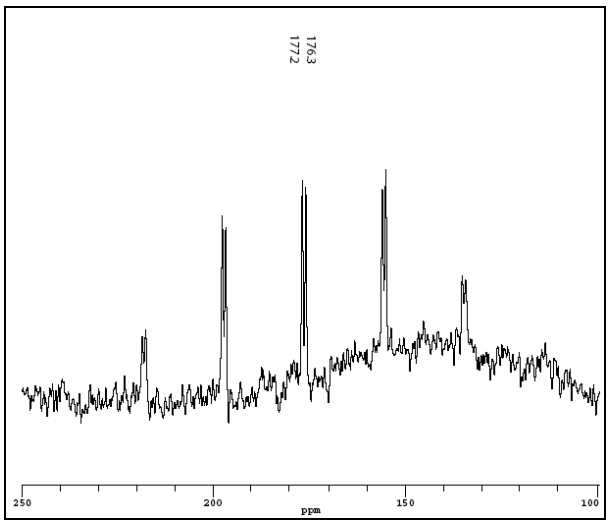

Sample Name	L-Leucine
MAS Frequency	3.1KHz
No. of Acquisitions	1024
Pulse Delay	3s
Acquisition Time	40ms
90° ^{1}H Pulse Length	2.5μs
Contact Time	2ms

Figure 11: L-Leucine spinning at 3.1KHz, carbonyl region

Figure 12 shows the asymmetry in spinning side-bands associated with the M2 peptide when spinning at 3.2KHz.

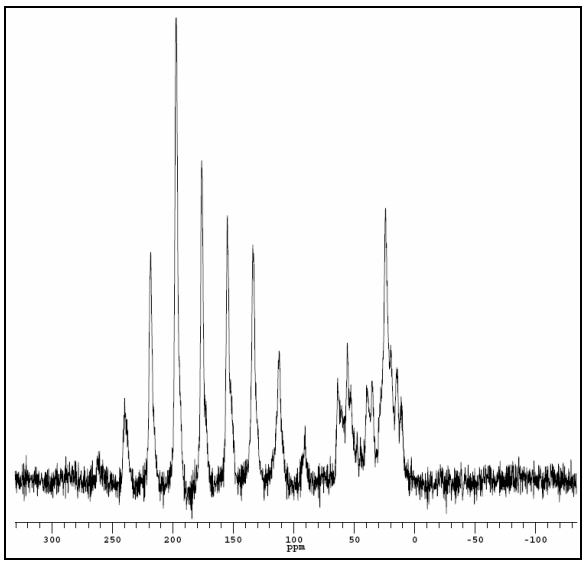

Sample Name	M2 peptide (AK02)
MAS Frequency	3.2KHz
No. of Acquisitions	320
Pulse Delay	1.5s
Acquisition Time	14.29ms
90° ^{1}H Pulse Length	2.5μs
Contact Time	2.5ms

Figure 12: M2 peptide at 3.2KHz

Figures 13 and 14 show the spectra from DPPC with two major carbonyl peaks, one with an additional shoulder. The two major peaks come from the two different C=O groups in the molecule (see Figure 2) and the shoulder at 174.6ppm is a result of the crystallisation of the DPPC.

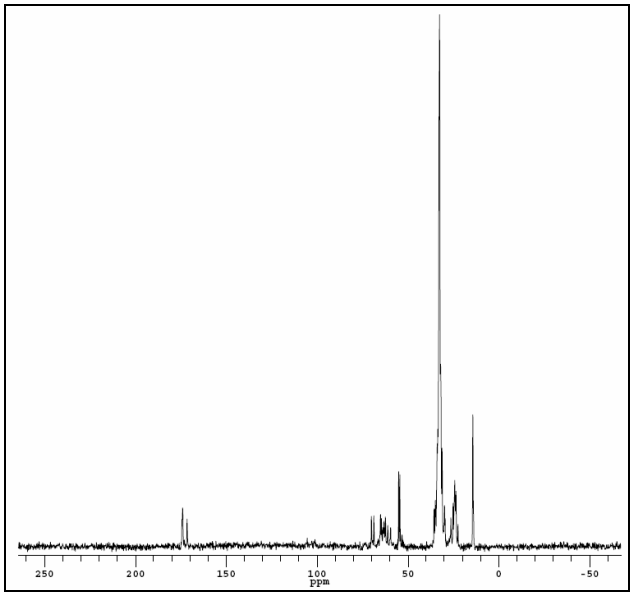

Sample Name	DPPC
MAS Frequency	10.3KHz
No. of Acquisitions	128
Pulse Delay	3s
Acquisition Time	20ms
90° ^{1}H Pulse Length	2.5μs
Contact Time	3ms

Figure 13: DPPC

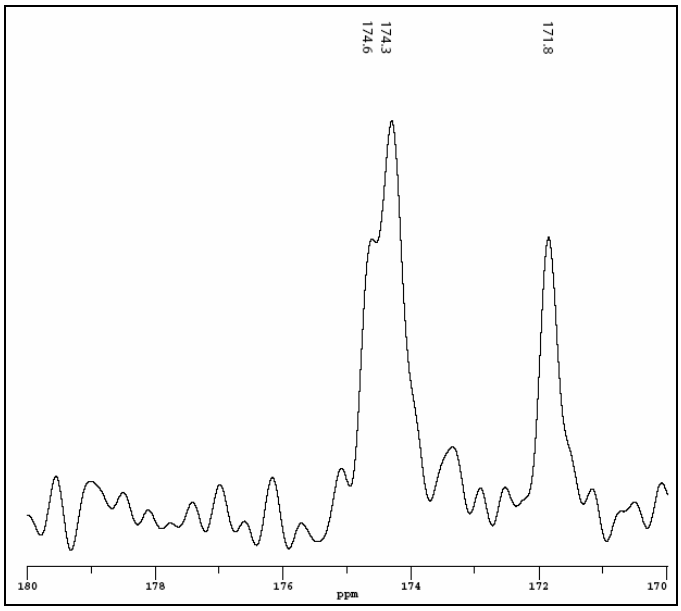

Sample Name	DPPC
MAS Frequency	10.3KHz
No. of Acquisitions	128
Pulse Delay	3s
Acquisition Time	20ms
90° ^{1}H Pulse Length	2.5μs
Contact Time	3ms

Figure 14: DPPC, expanded carbonyl region

Figures 15 and 16 show the spectra of the M2 peptide reconstituted into DPPC vesicles.

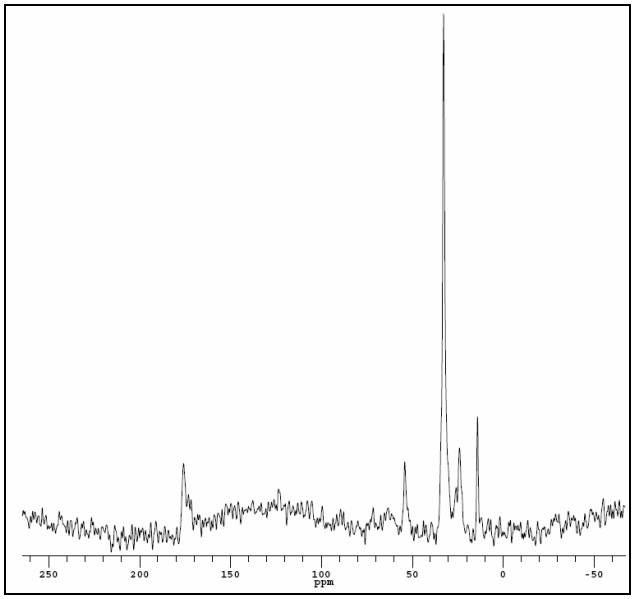

Sample Name	M2(AK02) + DPPC
MAS Frequency	10.3KHz
No. of Acquisitions	1024
Pulse Delay	3s
Acquisition Time	20ms
90° ^{1}H Pulse Length	2.5μs
Contact Time	3ms

Figure 15: M2 peptide reconstituted in DPPC

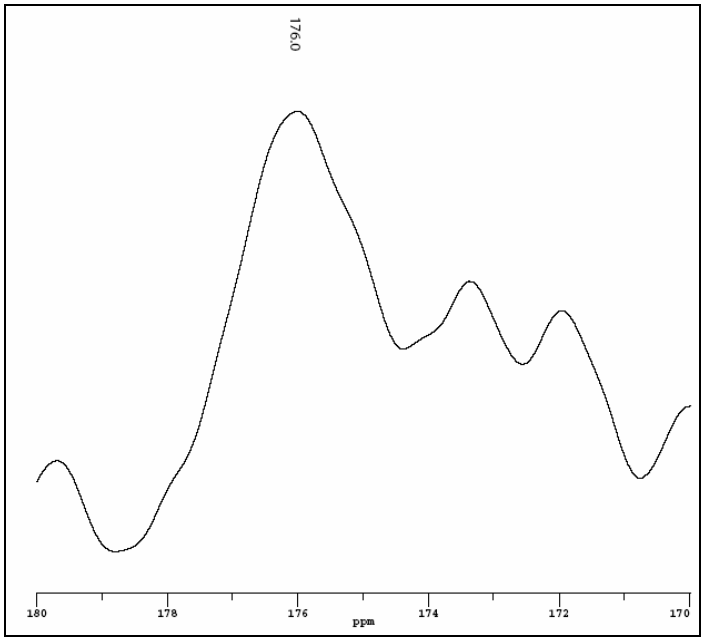

Sample Name	M2(AK02) + DPPC
MAS Frequency	10.3KHz
No. of Acquisitions	1024
Pulse Delay	3s
Acquisition Time	20ms
90° ^{1}H Pulse Length	2.5μs
Contact Time	3ms

Figure 16: M2 peptide reconstituted in DPPC, expanded carbonyl region

3.2 FTIR Spectra

Figure 17 shows the FTIR spectra of the purified M2 peptide (AK03) reconstituted in DPPC and Figure 18 shows the peak-fitting applied by a mixed Gaussian and Lorentzian algorithm.

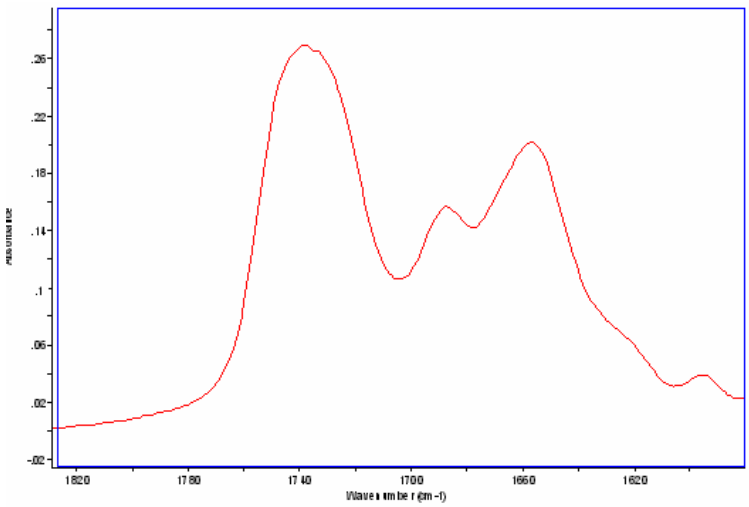

Figure 17: FTIR spectra of M2 (AK03) + DPPC

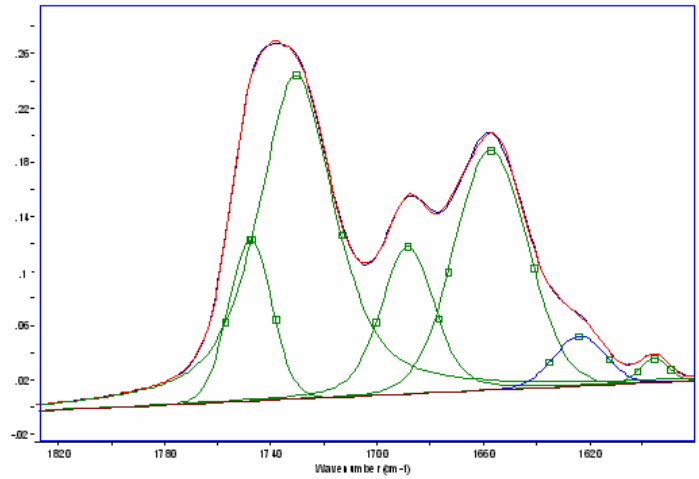

Figure 18: Peak fitting of M2 (AK03) + DPPC FTIR spectra

Peaks 1 and 2 (labelled left to right) show the absorbance of the DPPC in 2 conformations as a result of its crystallisation. The origin of peak 3 is a small amount of residual TFA. Peaks 4 is a result of the Amide 1 group on the peptide. The absorbance seen is about 20% caused by the

$^{12}C=^{14}N$ stretch vibrations and 80% from the carbonyl $^{12}C=^{16}O$ vibrations. The shoulder (peak 5) on the main peak (peak 4) is due to $^{13}C=^{18}O$ vibrations from the 1.1% natural abundance ^{13}C. The broadening evident in peak 5 is because some of the peptide is not in an α-helical formation. The areas under each peak directly correspond to the levels of substance in the sample and are given below in Table 1.

Table 1

Peak Number	Area Under Absorbance Curve
1	2.458
2	10.454
3	3.060
4	6.188
5	0.888
6	0.238

Peak 6 originates from the labelled $^{13}C=^{18}O$ groups in Leucine39 of the peptide. We would expect the area under peak 6 to be approximately 4% the size of the total peptide absorbance area (peaks 4,5 and 6). $\frac{Area\,6}{Area\,4 + Area\,5 + Area\,6} = \frac{0.238}{6.188 + 0.888 + 0.238} = 0.032$. Based on guidance from the manufacturer, we assume that ^{13}C is 99% pure and ^{18}O is 65% pure and the discrepancy we observe between the predicted 4% and the calculated 3.2% is because not all of the Leucine39 will have been correctly labelled.

4 Discussion

The aim of this work was to develop the methodology for solid-state NMR and IR studies of biological samples using a synthetic M2 peptide. To this end, a method has been achieved for successfully analysing the peptide in a purified powdered state and when it has been reconstituted in a lipid bilayer.

The peptide exhibits a strong NMR signal at 176.6ppm (Figures 8 and 9), which is in the region corresponding to the carbonyl groups in the isotopically labelled residues of the peptide. This confirms that the peptide is correctly labelled. The small shoulder seen on the right of the main peak (Figure 9) could be due to a signal from a small number of peptides that differ slightly in their amino acid sequence due to imperfections in the synthesis and purification methods used. This results in the labelled residue having a slightly different local environment and hence a different chemical shift. One pair of side-bands are evident as is a small signal in the 0-75ppm range from the natural abundance ^{13}C in other groups within the peptide. It was found that purifying the peptide via HPLC had a negligible effect on improving the NMR spectra in line with expectations as the synthesized peptide is assumed to be over 90% pure (manufacturers guidance).

The spectrum for L-Leucine (Figure 10) shows a natural abundance signal from the four different carbon groups in its structure. The doublet seen in the carbonyl region is due to a difference in local environments of the two C=O groups in the amino acid. A clear distinction can be seen between the symmetry of the side bands of the peptide (Figure 8) and the side bands of L-Leucine (Figure 11). This demonstrates the high resolution of NMR spectroscopy as it can differentiate between a residue embedded within the peptide and a residue isolated from other types of molecule. The chemical shifts at the carbonyl region were effectively the same with a peak at 176.6ppm for the peptide and peaks at 176.3 and 177.2ppm for the L-Leucine as expected.

DPPC exhibits its strongest NMR signal at 25.3ppm (Figure 15) which is a result of the carbons in the long hydrocarbon chain in the molecule. The carbonyl doublet (171.8 and 174.3ppm) corresponds to the two C=O groups in the molecule with the shoulder at 174.6ppm arising as a

consequence of the crystallisation of the lipid. The chemical shifts in the carbonyl region are lower than those observed for the M2 peptide which reflects the different local environments that the ^{13}C atoms are experiencing.

The spectrum of the peptide reconstituted in DPPC shown in Figure 16 displays a main carbonyl chemical shift peak at 176.0ppm which is in line with that expected from the peptide. The doublet giving a lower signal at a lower chemical shift is from the natural abundance ^{13}C in the lipid as seen in Figure 14. The signal observed in figures 8 and 9 shows that we have generated sufficient signal from the peptide, even when it is reconstituted in DPPC, to extract useful information from the sample. The peptide was mixed with the DPPC in a 1mg:6.7mg ratio which meant that there was less peptide that could be fitted inside the rotor and so being able to obtain a strong NMR signal is a significant result.

The gel-like samples where the peptide/lipid mixture had been hydrated in different quantities of water did not produce an NMR signal. This could either be due the sample being in too liquid a form to perform solid-state NMR or it may be due to not being able to get sufficient sample in the rotor with the additional inserts in place. This highlighted the difficulty of attempting to accurately mimic the environment of a membrane protein. Although embedding in a lipid bilayer does improve the accuracy of the model, it is important to develop some way of increasing fluidity as can be found typically within the virus' natural environment. Nishimura *et al*. (2002) have attempted to do this with some success by hydrating a peptide/lipid mixture and spinning it down using a centrifuge and performing solid-state NMR on the resulting pellet.

The FTIR spectra (Figures 16, 17) prove that the hydrated peptide/lipid mixture which did not give an NMR signal did in fact contain peptide and lipid in the correct ratio of quantities (see Table 1). FTIR requires a smaller amount of sample to operate than NMR although it does not elicit as high resolution structural information. While FTIR can provide some useful information on membrane proteins (Kukol *et al*., 1999), if enough signal can be generated, solid-state NMR provides the potential for far more detailed and wide-ranging structural information (Wang *et al*., 2001).

The natural extension of this work is to use other labels such as ^{15}N in combination with ^{13}C labels to measure dipole-dipole coupling at a specific site within the peptide. From the resulting spectra, it would be possible to accurately calculate a bond distance within the molecule. If we had 2 known bond distances within the molecule, these could be used as restraints in a computer modelling simulation using QUANTA (Accelrys, San Diego, USA) or a similar program to provide the most likely structure of M2 in the membrane.

The techniques and methodology developed here can be applied to other biological samples with, for example, ^{17}O labels which are considerably more expensive and on which a long process of methodology development is not financially viable.

5 Conclusion

This work has illustrated the potential power of solid-state NMR and IR spectroscopy as very local probes of molecular structure in biological systems. It has been demonstrated that small synthetic peptides can be successfully reconstituted into artificial lipid bilayers and still produce sufficient signal to perform solid-state NMR. Information has been gathered regarding the local environment of the carbonyl groups in the labelled Leucine36 and Leucine38 residues and it has been shown that this environment is different when embedded in a bilayer to when it is isolated from other types of molecule. This variation is exhibited in a change in the anisotropic chemical shift and in the asymmetry co-efficient of the NMR signal.

This work could be extended to further develop the methodology for solid-state NMR studies of biological samples, particularly in increasing the fluidity of the artificial bilayer to provide a more realistic environment for the transmembrane domain. Dipole-dipole coupling could then be used to establish intramolecular distances and these in turn could be employed as restraints in molecular simulations to provide accurate structural depictions of membrane proteins.

References

Arkin, I.T., MacKenzie, K.R. & Brunger, T. (1997). Site-directed dichroism as a method for obtaining rotational and orientational constraints for oriented polymers. *J. Am. Chem. Soc*., **119**, 8973-8980.

Bennett, A.E., Rienstra,, C.M., Auger, M., Lakshmi, K.V. & Griffin, R.G. (1995). Heteronuclear decoupling in rotating solids. *J. Chem. Phys*., **103**, 6951-6958

Brown, S.P. & Emsley, L. (2003). Solid-state NMR Article for: Handbook of Spectroscopy, Vo-Dinh, Gauglitz (eds.), Chichester, England: John Wiley & Sons Ltd.

Brown, S.P. & Spiess, H.W. (2001). Advanced Solid-State NMR Methods for the Elucidation of Structure and Dynamics of Molecular, Macromolecular, and Supramolecular System. *Chem. Rev*., **101**, 4125-4155.

Duff, K., Kelly, S., Price, N. & Bradshaw, J. (1992). The secondary structure of influenza A M2 transmembrane domain. A circular dichroism study. *FEBS Letters*, **311**, **(3)**, 256-258

Fischer, W.B. & Sansom, M.S.P. (2002). Viral ion channels: structure and function. *Biochimica et Biophysica Acta*, **1561**, 27-45

Hay, A., Wolstenhome, A., Skehel, J. & Smith, M. (1985). The molecular basis of the specific anti-influenza action of amantadine. *EMBO J*. **4 (11)**, 3021-3024

Holsinger, L., & Lamb, R. (1991). Influenza virus M2 integral membrane protein is a homotetramer stabilized by formation of disulfide bonds. *Virology*, **183**, **(1)**, 32-43

Jeschke, G. (2003). High-resolution solid-state NMR in Structure Determination II. Chichester, England: John Wiley & Sons Ltd.

Kochendoerfer, G.G., Salom, D., Lear, J.D., Wilk-Orescan, R., Kent, S.B. & DeGrado, W.F. (1999). Total chemical synthesis of the integral membrane protein *Influenza A* virus M2: role of its C-terminal domain in tetramer assembly. *Biochemistry*, **38 (37)**, 11905-11913.

Kukol, A., Adams, P.D., Rice, L.M., Brunger, A.T. & Arkin, I.T. (1999). Experimentally based orientational refinement of membrane protein models: a structure for the *Influenza A* M2 H^+ Channel. *J. Mol. Biol.*, **286**, 951-962.

Levitt, M.H. (2000). Spin Dynamics: Basics of Nuclear Magnetic Resonance. Chichester, England: John Wiley & Sons Ltd

Lowe, I.J. (1959). Free induction decays of rotating solids. *Phys. Review. Letters*, **2**, 285-287

Nidus Information Services (2001). Specific drugs for treating and preventing severe influenza, http://www.ucdmc.ucdavis.edu/ucdhs/health/a-z/94ColdsInfluenza/doc94medictreatprev.html, University of California, Davis

Nishimura, K., Kim, S., Zhang, L. & Cross, T. (2002). The closed state of a H^+ channel helical bundle combining precise orientational and distance restraints from solid state NMR. *Biochemistry*, **41**, 13170-13177

Otzen, D.E. (2004). Membrane protein biophysics, http://www.inano.dk/sw1400.asp, University of Aarhus

Press, W.H., Flannery, B.P., Teukolsky, S.A. & Vetterling, W.T. (1986). Numerical recipes, Cambridge, England: Cambridge University Press, 521-528.

Hoffman-La Roche Ltd. (2004). Influenza viruses alter their surface proteins, http://www.roche.com/pages/facets/10/viruse.htm, Hoffman-La Roche Ltd.

Torres, J., Kukol, A., Goodman, J.M. & Arkin, I.T. (2001) Site-specific examination of secondary structure and orientation determination in membrane proteins: the peptidic $^{13}C=^{18}O$ group as a novel infrared probe. *Biopolymers*, **59(6)**, 396-401

Wang, J., Sanguk, K., Kovacs, F. & Cross, T.A. (2001). Structure of the transmembrane region of the M2 protein H^+ channel. *Protein Science*, **10**, 2241-2250

World Health Organisation (2003). Influenza, http://www.who.int/mediacentre/factsheets/fs211/en, World Health Organisation

Appendix

Amino acid sequence of M2 protein

MSLLTEVETPIRNEWGCRCNDSSDPLVVAASIIGILHLILWILDRLFFKCIYRFFEHGLKRG
PSTEGVPESMREEYRKEQQSAVDADDSHFVSIELE

Amino acid sequence of synthetically generated M2 transmembrane peptide

SSDPLVVAASIIGI[1]L[2]HL[3]I[4]LWILDRL

Where indicated the $^{13}C=^{18}O$ labels are as follows,

AK01: Isoleucine

AK02: Leucine

AK03: Leucine

AK04: Isoleucine

Abbreviations

ATP: Adenosine tri-phosphate

CD: Circular dichroism

CP: Cross-polarisation

DPPC: 1,2-dipalmitoly-sn-glycero-3-phosocholine

FTIR: Fourier transform infra-red spectroscopy

HPLC: High performance liquid chromatography

IR: Infra-red spectroscopy

MAS: Magic angle spinning

NMR: Nuclear magnetic resonance

ppm: Parts per million

RNA: Ribonucleic acid

RNP: Ribonucleoprotein

SSID: Site-specific infra-red dichroism

TFA: Trifluoroacetic acid

TPPM: Two pulse phase modulation